RSC Advances

ROYAL SOCIETY OF CHEMISTRY

www.rsc.org/advances

Journal Name

ARTICLE

Synthesis, characterization and micellization of amphiphilic polyethylene-*b*-polyphosphoester block copolymers

Received 00th January 20xx,
Accepted 00th January 20xx

DOI: 10.1039/x0xx00000x

www.rsc.org/

Haiyang Gao*, Yinxin Tan, Qirui Guan, Tao Cai, Guodong Liang, and Qing Wu

A sequential synthetic strategy combining metal catalyzed living polymerization of ethylene and ring-opening polymerization (ROP) was successfully used to prepare novel polyethylene-*block*-polyphosphoester (PE-*b*-PPE) diblock copolymers. Narrowly dispersed hydroxyl-terminated polyethylene (PE–OH) was firstly synthesized by amine-imine nickel catalyzed-living polymerization of ethylene and subsequent chain transfer reaction. PE-*b*-PPE diblock copolymers with narrow polydispersities were obtained by organocatalyzed ring-opening polymerization (ROP) of 2-ethyoxyl-2-oxo-1,3,2-dioxaphospholane or 2-methyl-2-oxo-1,3,2-dioxaphospholane using PE–OH as a macroinitiator. Investigations of self-assembly of the obtained PE-*b*-PPEs block copolymers in water by means of TEM and laser light scattering confirmed that the amphiphilic block copolymers formed micelles in aqueous solution. These PE-*b*-PPE block copolymers was used for paclitaxel (PTX) encapsulation to demonstrate the potential in drug delivery. These biocompatible PE-PPE polymeric micelles showed high loading efficiency of 92% and content of PTX of 16.6 wt% as well as slow and sustained release behavior.

Introduction

Polyolefins, especially polyethylene (PE), are commercially the most important family of polymers.[1] Although polyolefins have reached wide application, their applications are mainly limited to the field of plastic and resin due to their low polarity and poor reactivity.[2-4] Development of functional polyolefin materials is of significant academic and industrial interest and still remains a longstanding challenge. Current advance shows that a few functional polyolefin copolymers such as PE-*b*-PS, PE-*b*-PMMA, and PE-*b*-PCL (poly(ε-caprolactone)) have been successfully synthesized and show important application in the field of compatibilizers for polymer blends and nanoporous membranes.[5-8] Few polyolefin based amphiphilic copolymers have been prepared,[9-12] although amphiphilic copolymer can self-assemble into various nanostructures, which have many potential applications in the areas of drug delivery, biomaterials, sensors, and electronics.[13-15]

Main limitation for synthesis of well-defined polyolefin based amphiphilic copolymers is poor solubility and reactivity of polyolefin block, which largely restricts occurrence of chain extension reaction. Reducing molecular weight of polyolefin is a viable access to synthesis of polyolefin based amphiphilic copolymer. Several noteworthy examples are polyolefin-*b*-polypeptide,[16-18] PE-*b*-PEO,[19] and polyethylene-*b*-poly(*N*-isopropylacrylamide) (PE-*b*-PNIPAM) block copolymers,[20] the low-molecular-weight of hydrophobic polyolefin building blocks (M_n < 5 kg/mol) are obtained by anionic living polymerization of diene or coordination chain transfer polymerization (CCTP).[16-20] Besides, the approach of increasing branching density or changing polymer topology by late transition metal catalyzed olefin polymerization can also improve solubility of polyolefin in organic solvents.[9-12,21-27] Highly branched polyethylene with high molecular weight obtained by α-diimine palladium catalyst can be used to construct amphiphilic copolymer, and novel PE based amphiphilic copolymers have been developed.[9-12] A type of nickel catalyst bearing amine-imine ligand has been recently developed for living polymerization of ethylene to afford branched PE.[28-32] Living polymerization of ethylene and subsequent chain transfer reaction can afford end-functionalized PE, which can be used to construct PE based amphiphilic block copolymers in combination with other controlled polymerization.[22,23]

Polyphosphoestes are of particular interest (PPEs) because of their favorable biocompatibility, biodegradability, and relatively controllable hydrophilicity, and their potential applications in biomedical applications.[33-36] Construction of polyphosphoester based amphiphilic copolymers by introduction of other building block can not only enrich this class of biocompatible polymer materials but also allow for adjustable physical and chemical properties.[37-39] To our best knowledge, no amphiphilic polyolefin-polyphosphoester block copolymer has been reported up to now. In this paper, we report the synthesis and characterization of novel amphiphilic polyethylene-*block*-polyphosphoester (PE-*b*-PPE)

PCFM Lab, GD HPPC Lab, DSAPM Lab, Institute of Polymer Science, School of Chemistry and Chemical Engineering, Sun Yat-Sen University, Guangzhou 510275, China. E-mail: gaohy@mail.sysu.edu.cn; Fax: 86-20-84114033; Tel: 86-20-84113250.

† Footnotes relating to the title and/or authors should appear here.
Electronic Supplementary Information (ESI) available: [Synthetic routes and NMR spectra of monomers, synthesis and characterization of TU.]. See DOI: 10.1039/b000000x/.

diblock copolymers. The self-assembly, thermal responsibility, and encapsulation property toward hydrophobic molecules of PE-*b*-PPE copolymers in aqueous solution were further studied for a better understanding of potential applications of this kind of novel block copolymers.

Results and Discussion

Synthesis and characterization of PE-*b*-PPE diblock copolymers

PE-*b*-PPE diblock copolymers were synthesized by a sequential synthetic strategy combining metal catalyzed living polymerization of ethylene and ring-opening polymerization (ROP) of 2-ethyoxyl-2-oxo-1,3,2-dioxaphospholane (EEP) and 2-methyl-2-oxo-1,3,2-dioxaphospholane (MeEP) (Scheme 1). The first challenge was how to synthesize narrowly dispersed hydroxyl-terminated polyethylene as a macroinitiator. Hydroxyl-terminated polyethylenes with low molecular weight were previously prepared by coordination chain transfer polymerization (CCTP) using specific catalytic systems.[40-42] However, the linear PE obtained by these catalytic systems has poor solubility in solvents, which limits occurrence or controlled fashion of chain extension reaction. Our previous study has shown that amine-imine nickel catalyst 1 (see Scheme 1) can polymerize ethylene in a living fashion to afford highly branched PE with good solubility in organic solvents.[28-32] The macroinitiator PE–OH with high molecular weight can be thereby prepared by amine-imine nickel-catalyzed ethylene living polymerization and subsequent chain transfer to $ZnEt_2$.[22] The structure of hydroxyl terminated PE (PE–OH) was characterized to has M_n of 19 kg/mol, M_w/M_n of 1.03, branching density of 81/1000C determined by ^{1}H NMR and end functionality of ~92% by ratio of absolute M_n determined by GPC with a light scattering (LS) detector to the data detected by the ^{1}H NMR spectrum.

Scheme 1 Synthesis of PE-*b*-PPE diblock copolymers.

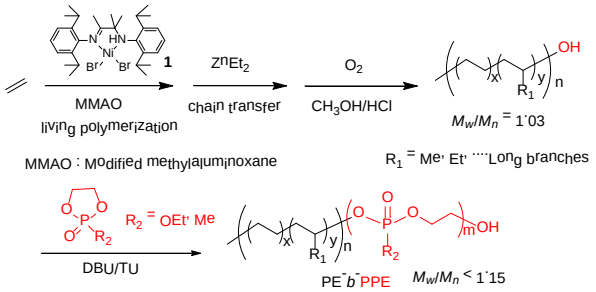

Higher molecular weight PE–OH is hardly characterized by ^{1}H NMR, and its poor solubility also enhance difficulty of sequential chain extension reaction. Therefore, the hydroxyl end group of the obtained PE–OH with M_n of 19 kg/mol was used to initiate the ROP of 2-ethyoxyl-2-oxo-1,3,2-dioxaphospholane (EEP) and 2-methyl-2-oxo-1,3,2-dioxaphospholane (MeEP) to afford block copolymers. According to previous reports, the $Sn(Oct)_2$ catalytic system can control the ROP of cyclic phosphate monomers well to produce linear polyphosphoesters at the mild temperature using low molecular weight alcohol as initiator.[35,43-46] However, our experimental result showed that the ROP of EEP using $Sn(Oct)_2$ as catalyst and high-molecular-weight PE–OH as macroinitiator produced polymer with broad molecular weight distribution (M_w/M_n = 1.65). Iwasaki has reported that some organocatalysts can conduct the ROP of cyclic phosphate monomers to afford linear well-defined polyphosphates with narrow molecular weight distribution.[36,47-50] In our experiments, organocatalyzed ROP was successfully applied to construct block copolymer in a controlled fashion. A crucial issue for achievement of controlled ROP is to conduct polymerization at suitable EEP monomer concentration. Usually, high EEP monomer concentration leads to precipitation of macroinitiator PE–OH because of increasing polarity of reaction system, while low EEP monomer concentration causes loss of controlled fashion because of occurrence of intra-, or inter-molecular transesterification reaction.[51] Three samples of polyethylene-*block*-poly(ethyl ethylene phosphate) (PE-*b*-PEEP) copolymers were synthesized using 1,8-diazabicyclo[5.4.0]undec-7-ene/thiourea (DBU/TU) as organocatalyst at EP concentration 1.21 M, and the block length of the polyphosphate segment could be controlled by tuning reaction time (Table 1). Similarly, three samples of polyethylene-*block*-poly(ethylene methylphosphonate) (PE-*b*-PMeEP) copolymers were precisely synthesized using single DBU as organocatalyst at low MeEP concentration ($[M]_0/[I]_0$ = 200) because of no transesterification reaction (Table 1).[52]

Table 1 Synthesis of and characterization of PE-*b*-PPE copolymers.

Entry	Copolymers	$[M]_0/[I]_0$ [a]	t (h)	$M_{n\text{-}PPE}$ [b]	$M_{n\text{-}NMR}$ [b]	$M_{n\text{-}GPC}$ [c]	M_w/M_n [c]
1	PE_{680}-*b*-$PEEP_{33}$	800	1.0	5.0	24.0	22.5	1.10
2	PE_{680}-*b*-$PEEP_{131}$	800	3.5	19.9	38.9	32.6	1.12
3	PE_{680}-*b*-$PEEP_{170}$	800	4.5	25.9	44.9	41.2	1.15
4	PE_{680}-*b*-$PMeEP_{47}$	200	1.0	5.6	24.6	23.5	1.07
5	PE_{680}-*b*-$PMeEP_{73}$	200	1.5	8.8	27.8	27.3	1.09
6	PE_{680}-*b*-$PMeEP_{112}$	200	2.0	13.4	32.4	31.8	1.11

Polymerization conditions of ROP of EEP: 5 °C, 5.3 μmol macroinitiator PE–OH (M_n = 19 kg/mol, M_w/M_n = 1.03), DBU/TU=1:1, 0.106 mmol, THF as solvent, total volume: 3.5 mL. Polymerization conditions of ROP of MeEP: 5 °C, 6.2 μmol macroinitiator PE–OH, 0.125 mmol DBU, $CHCl_3$ as solvent, total volume: 3.5 mL. [a] Ratio of monomer to macroinitiator PE–OH. [b] In unit of kg/mol, determined by ^{1}H NMR. [c] Determined by gel permeation chromatography (GPC) in CH_3Cl.

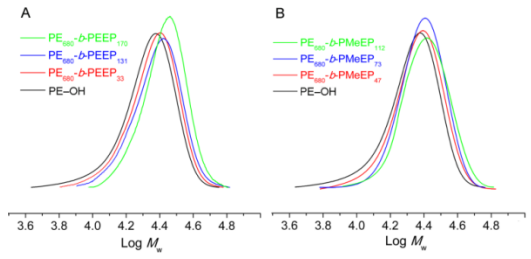

Figure 1 GPC profiles of PE-*b*-PEEP (A) and PE-*b*-PMeEP (B) copolymers.

The PE-*b*-PPE block copolymers were obtained by dialysis for removal of organic small molecule compounds and purification from ethanol to remove small amount of PE homopolymer. The

molecular weights and molecular weight distributions of copolymers were measured by GPC using a good solvent of chloroform as eluent. As shown in Figure 1, GPC profiles of PE-*b*-PEEP and PE-*b*-PMeEP copolymers are monomodal and symmetric and no tail or shoulder peaks are observed, suggesting that pure PE-*b*-PEEP and PE-*b*-PMeEP block copolymers were obtained without homopolymers. The number-average molecular weight (M_n) of PE-*b*-PEEP and PE-*b*-PMeEP block copolymers grows with increasing polymerization time of ROP and M_w/M_n values are below 1.15 (see Table 1), proving successful polymerization of cyclic phosphoester monomers and formation of copolymer in such conditions.

The chemical structure of PE-*b*-PEEP copolymer can be identified by the ^{1}H NMR spectrum. In comparison with the ^{1}H NMR spectrum of PE–OH in Figure 2, the new signals are clearly observed at 4.0-4.5 ppm in the ^{1}H NMR spectra of PE-*b*-PEEP copolymers, which can be separately assigned to the protons of –OCH_2–CH_2O– and –OCH_2CH$_3$ in the PEEP block. Disappearance of a characteristic peak at 3.65 ppm (PE–CH_2OH) indicates full removal of macroinitiator. Moreover, the peak intensity at 4.0-4.5 ppm of the copolymer obviously increases with prolonging polymerization time, suggesting that PEEP block length increase. The number-average molecular weights (M_n) of PE-*b*-PEEP block copolymers are also calculated by integral ratio of characteristic peak in ^{1}H NMR spectrum in combination with absolute M_n of PE determined by GPC-LS. Apparently, the molecular weight results determined by GPC are reasonably consistent with those of ^{1}H NMR analysis.

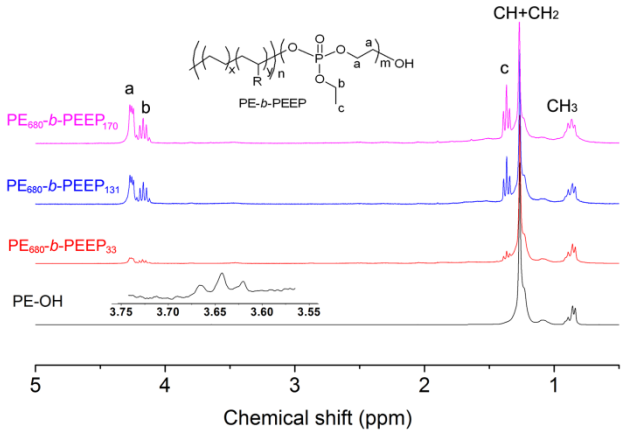

Figure 2 ^{1}H NMR spectra of PE–OH and PE-*b*-PEEP in $CDCl_3$.

The chemical structure of PE-*b*-PMeEP is also confirmed by the ^{1}H NMR spectrum.[52] In Figure 3, the characteristic split peak at 1.58 ppm can be assigned to side methyl group (P–CH_3). The broad resonance observed at 4.28-4.23 ppm can be attributed to the protons of –OCH_2–CH_2O–. The linkage of PE block and PMeEP block can be safely proved on the basis of presence of weak resonance at 3.81 ppm (PE–CH_2O–PMeEP), and the end group of CH_2OH can be observed at 3.71 ppm.

The ^{13}C NMR spectra of copolymers shown in Figure 4 are also found to be in accord with the expected chemical structure of the block copolymers. In contrast to the ^{13}C NMR spectrum of PE–OH, three new signals which emerged at 66.23, 64.51, and 16.02 ppm in the ^{13}C NMR spectrum of PE_{680}-*b*-$PEEP_{131}$ are attributed to the carbons of –OCH_2–CH_2O–, –OCH_2CH$_3$–, and –OCH$_2$CH_3–, respectively. From the ^{13}C NMR spectrum of PE_{680}-*b*-$PMeEP_{47}$ copolymer, the peak at 64.71 ppm can be assigned to the carbons of –OCH_2–CH_2O– and the characteristic split peak at 10.69 ppm can be assigned to the side methyl group.

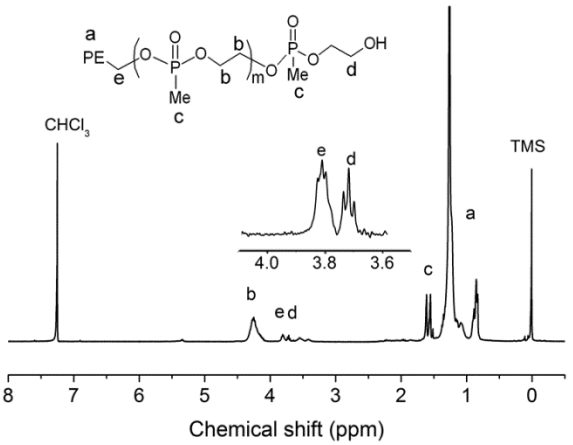

Figure 3 ^{1}H NMR spectrum of PE_{680}-*b*-$PMeEP_{47}$ copolymer in $CDCl_3$.

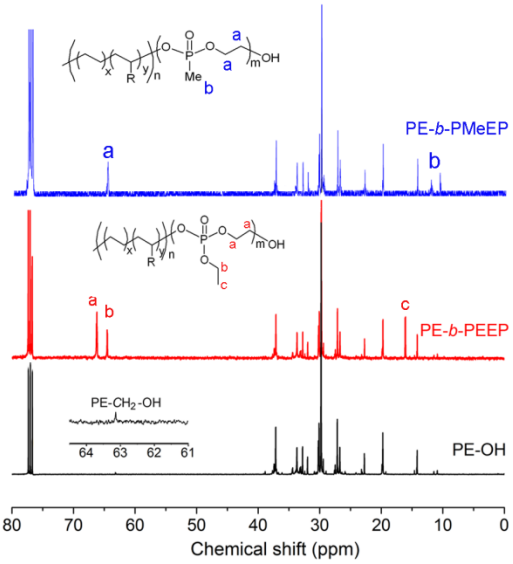

Figure 4 ^{13}C NMR spectra of PE–OH and PE-*b*-PPE copolymers (entries 2 and 4).

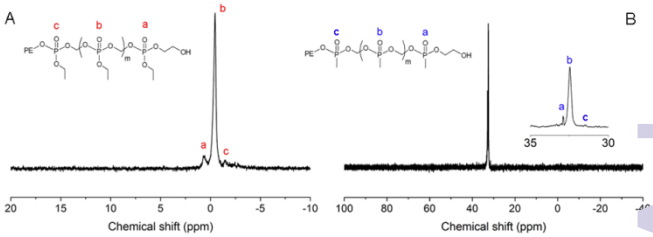

Figure 5 ^{31}P NMR spectra of PE-*b*-PPE copolymers (entries 2 and 4).

^{31}P NMR spectra of PE-*b*-PPE copolymers also further support successful incorporation of PPE blocks (Figure 5). For the ^{31}P NMR spectrum of PE-*b*-PEEP copolymer, a strong resonance at -0.46 ppm is assigned to phosphorous atoms of PEEP block, which is different to monomer signal of 18.48 ppm (see Figure S2 in Supporting

Information (SI)). Two weak resonances emerged at 0.73 and -1.46 ppm can be attributed to end phosphorous atoms of PEEP block. For the ^{31}P NMR spectrum of PE-*b*-PMeEP copolymer, a strong resonance at 32.47 ppm is assigned to phosphorous atoms of PMeEP block, which is different to monomer signal of 48.78 ppm (see Figure S4 in SI). Two weak resonances at 32.91 and 31.90 ppm are attributed to end phosphorous atoms of PMeEP block.

Self-assembly of PE-*b*-PPE copolymers in aqueous solution

PE-*b*-PPE copolymers are consisted of hydrophobic PE segments and hydrophilic PPE segments. Amphiphilic block copolymers have been found to self-assemble spontaneously into polymeric aggregates in selective solvents. Previous study show that PE based amphiphilic copolymers can self-assemble into spherical micelle, nanodisk-like micelle, unimolecular micelle, and vesicle morphologies in aqueous solution.[9-12,19-27] In this study, self-assembly of PE-*b*-PPE copolymers in water was investigated, which is interesting and helpful for a better understanding of potential application in encapsulating hydrophobic drug.

Aqueous solutions of six amphiphiles were prepared by dialysis of their solutions in THF against water, and the dialysate was replaced several times by water to ensure a complete exchange of solvents. First, the critical aggregation concentrations (CAC) of the block copolymers were determined using pyrene as a fluorescent probe. Solutions of PE-*b*-PPE copolymers with concentrations ranging from 0.004 to 0.1 mg/mL were prepared with a constant pyrene concentration of 1×10^{-6} mol/L. The I_I/I_{III} band intensity ratios of the pyrene emission are typically plotted against logarithm of the PE_{680}-*b*-$PEEP_{33}$ polymer concentration in Figure 6, and a deflection point at its CAC of 0.015 mg/mL was observed. The low CAC value corresponds to 6.25×10^{-7} mol/L, which is a result of perfect hydrophobicity of PE building block. It is observed that CAC value increased with an increasing length of PPE block (Table 2) because high hydrophilic fraction results in weaker interactions between hydrophobic chains, thus leading to increase CAC value to achieve a more stable structure. Generally, PE-*b*-PPE micelles would thermodynamically stable in aqueous solution, and lower CAC value is surely favorable for drug delivery.

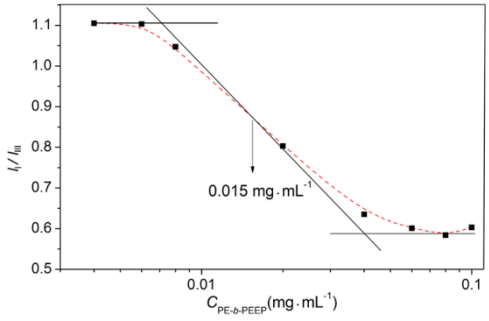

Figure 6 I_I/I_{III} ratios from the pyrene emission spectra *versus* the logarithm of PE_{680}-*b*-$PEEP_{33}$ concentration.

The self-assembly properties of PE-*b*-PPE block copolymers in aqueous solution were further studied by dynamic light scattering (DLS). Dynamic light scattering (DLS) measurements at 25 °C and 0.10 mg/mL for aqueous solution of PE-*b*-PEEP samples shows that the average hydrodynamic diameters (D_h) are in the range from 88 to 110 nm with unimodal size distributions of 0.115-0.134 (Table 2), suggesting an aggregation of the polymer chains. It is observed that D_h of PE-*b*-PEEP polymeric aggregates decreases from 110 to 88 nm with an increase in hydrophilic PEEP content, which is in good agreement with the one observed for other amphiphilic block copolymers as described by Discher and Eisenberg.[53-54] DLS measurements of PE_{680}-*b*-$PMeEP_{47}$ polymer samples show that the average hydrodynamic diameters (D_h) are smaller than those of PE_{680}-*b*-$PEEP_{33}$ polymeric aggregates although two polymers have nearly same PE/PPE weight ratio, which results from higher hydrophilicity of PMeEP chain. Similarly, PE-*b*-PMeEP polymeric micelles become small with increasing PMeEP block length.

Table 2 Self-assembly and PTX loading of PE-*b*-PPE copolymers.

Copolymers	PE/PPE [a]	CAC [b]	D_h [c] (nm)	PDI	D [d] (nm)	LE (%) [e]
PE_{680}-*b*-$PEEP_{33}$	79/21	0.015	110	0.115	100	92
PE_{680}-*b*-$PEEP_{131}$	49/51	0.022	92	0.122	84	85
PE_{680}-*b*-$PEEP_{170}$	42/58	0.024	88	0.134	81	81
PE_{680}-*b*-$PMeEP_{47}$	77/23	0.016	98	0.089	96	90
PE_{680}-*b*-$PMeEP_{73}$	68/32	0.018	94	0.098	91	83
PE_{680}-*b*-$PMeEP_{112}$	59/41	0.021	89	0.142	83	80

[a] Weight ratio of PE to PPE in copolymer, calculated from ^{1}H NMR. [b] Critical aggregation concentration (mg/mL), determined using pyrene as a fluorescent probe. [c] Average hydrodynamic radius, determined by DLS. Test conditions: 25°C, 0.1 mg/mL in water for PE-*b*-PEEP copolymers, and 25 °C, 0.1 mg/mL in water for PE-*b*-PMeEP copolymers. [d] Average radius of micelles obtained by TEM images. [e] Loading efficiency of PTX = (amount of PTX in the polymeric micelles/initial amount of the PTX) × 100, which was determined under the concentration of PTX 10 wt%.

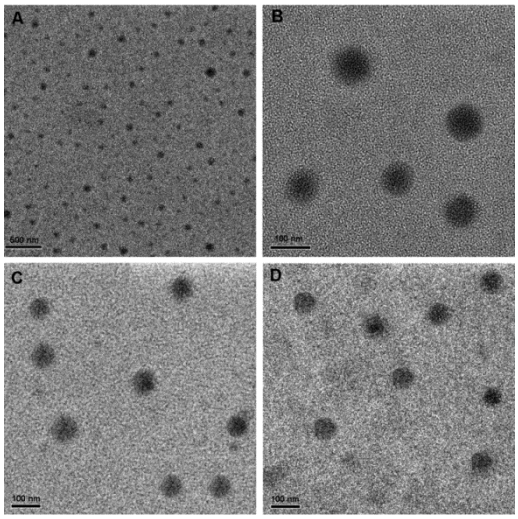

Figure 7 TEM images of polymeric micelles of PE-*b*-PEEP copolymers (A: PE_{680}-*b*-$PEEP_{33}$; B: magnified image of PE_{680}-*b*-$PEEP_{33}$; C: PE_{680}-*b*-$PEEP_{131}$; D: PE_{680}-*b*-$PEEP_{170}$).

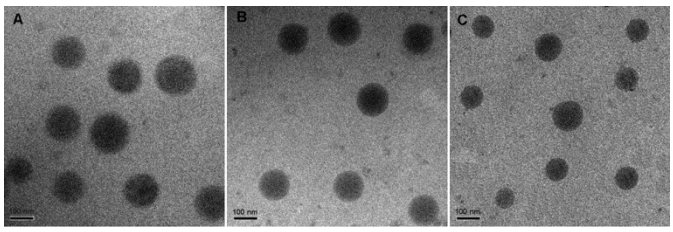

Figure 8 TEM images of polymeric micelles of PE-*b*-PMeEP copolymers (A: PE_{680}-*b*-$PMeEP_{47}$; B: PE_{680}-*b*-$PMeEP_{73}$; C: PE_{680}-*b*-$PMeEP_{112}$).

Transmission electron microscopy (TEM) was used to directly visualize the self-assembled nanostructures of block copolymers in water, and the successful formation of aggregates by the dialysis method was further confirmed by TEM measurements. Figure 7A clearly shows that PE_{680}-*b*-$PEEP_{33}$ amphiphiles in aqueous solution can self-assemble to form spherical micelles with uniform size (Figure 7A). The average diameters measured on the images (Figures 7B, C, and D) also show reducing trend with an increase in PEEP chain length, which is same to the results determined by DLS. Figure 8 shows that three PE-*b*-PMeEP amphiphiles in aqueous solution can also self-assemble into spherical micelles. The average diameters measured on the images are reasonably smaller than the data determined by DLS analysis, which is a result of differences of measurement state.

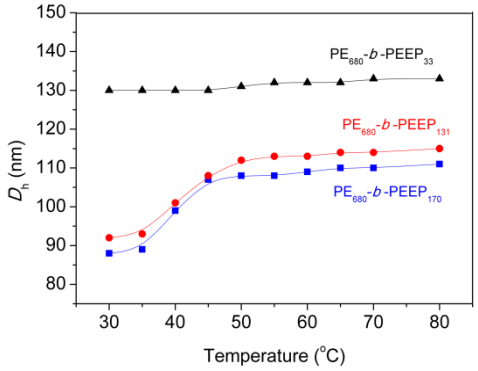

Figure 9 Plots of hydrodynamic diameter (D_h) *versus* temperature for PE-*b*-PEEP polymeric micelles.

Thermoresponsivity of PE-*b*-PPE polymeric micelles

As a thermo-responsive polymer, the incorporation of PEEP chain is expected to confer "thermo-sensitive" property on the PE-*b*-PEEP polymeric micelles. DLS measurement was performed to investigate a temperature dependence of hydrodynamic diameter (D_h) of the PE-*b*-PEEP block copolymer aggregates. When the degree of polymerization of PEEP chain was 33, the D_h was nearly unchanged in a temperature range from 25 to 80 °C and no detectable LCST was observed. When the degree of polymerization of PEEP chain increased up to 131, the obvious varieties of D_h were detected. As shown in Figure 9, D_h value of micelles was almost constant when the temperature was below 35 °C, and then a significant increase was observed in a temperature range from 35 to 50 °C. Two deflection points at lower critical solution temperatures (LCST) of 44 and 40 °C were observed for PE_{680}-*b*-$PEEP_{131}$ and PE_{680}-*b*-$PEEP_{170}$, respectively. Increasing PEEP block length leads to decreasing LCST, which is consistent previous observation.[45] Moreover, PE-*b*-PEEP block copolymers show increasing LCST relative to PEEP homopolymer (38 °C), [36] which is a result of incorporation of hydrophobic PE. However, no detectable LCSTs were observed for three PE-*b*-PMeEP block copolymers in aqueous solution by measurement of D_h at 15 to 90 °C and PE-*b*-PMeEP block copolymers could not exhibit thermo-responsibility. This observation is a result of good water solubility of PMeEP chain, and is well consistent with previous observation that no detectable LCST was detected for PMeEP homopolymer in aqueous solution up to 90 °C.[52]

Paclitaxel encapsulation into PE-*b*-PPE polymeric micelles

The hydrophobic core, hydrophilic shell structure of the PE-PPE polymeric micelles provides an ideal environment for encapsulati hydrophobic molecules. Paclitaxel (PTX), a powerful hydrophobic anticancer drug, was typically used to elevate this encapsulation ability of PE-PPE copolymer in aqueous solution, which would explore functional polyolefin in non-resin applications. To encapsulate the hydrophobic PTX, a solution of PTX in THF was mixed with a solution of PE-PPE block polymer and was then performed by dialysis of the THF solution against water. During micelles formation, the hydrophobic PTX molecules associated with the hydrocarbon structure of PE building block and became entrapped in the hydrophobic cores of the micelles. As expected, PTX loading was highly efficient for PE-PPE polymeric micelles. For example, PTX loading efficiency (LE) of PE_{680}-*b*-$PEEP_{31}$ reached 92% under the concentration of PTX 10 wt%. Increasing hydrophilic PPE fraction leads to a decrease in loading efficiency of PTX, which can be ascribed to reducing polymer aggregation number per micelle. The influence of concentrations of PTX on loading content of PTX was further studied with PE_{680}-*b*-$PEEP_{131}$ as a representative. As shown in Figure 10A, loading content of PTX (wt%) increase with an increase in concentration of PTX. Maximum loading content of PTX (16.6 wt%) occurred with 20 wt% concentrations of PTX. The drug loading efficiencies and contents into these PE-*b*-PPE micelles are much higher than that of other micellar systems in the reported literatures[55-59] and is comparable with microfluidic-assisted self-assembly of complex dendritic polyethylene drug delivery nanocapsules.[14] The high PTX loading efficiencies of PE-PPE polymeric micelles can be attributed to excellent hydrophobic environment of PE core. The morphology of PTX-loaded system is also spherical micelle, and no significant change of the size of micelles was observed despite the high PTX loading efficiencies, suggesting negligible interfere of PTX drug with self-assembly of block copolymer (see Figure S6 in SI).

In vitro release behavior of PTX was studied and performed in PBS (phosphate buffered solution, pH = 7.4) at 37 °C. As shown in Figure 10B, a slow and sustained release lasting long time from these PE-*b*-PPE polymeric micelles after relatively fast releases during the early stage (2 day) was observed, and about 77-93% of the initial loading content was eventually released, which is obviously higher than the value of PCL-*b*-PPE polymeric micelles

(45-75%).[57-59] Figure 10B also demonstrates that increasing PPE length leads to a relatively slower release because increasing hydrophilic block length would result in small dimension micelles with decreasing polymer aggregation number.

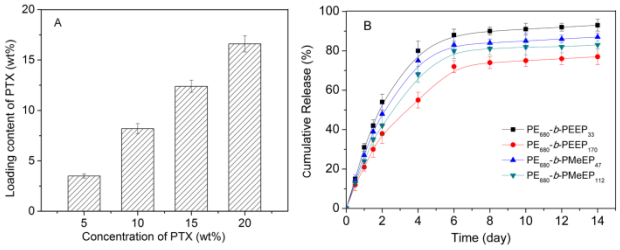

Figure 10 (A) Influence of concentration of PTX on loading content (mean ± SD, n = 3 independent experiments); (B) Release profile of PTX from PE-*b*-PPE polymeric micelles in PBS (pH = 7.4) at 37 °C.

In virtro cytotoxicity

It is reported that PPE are biocompatible, and PE is also nontoxic.[14,33-36] Therefore, PE-*b*-PPE copolymers were expected to be good biocompatibility. The cytotoxicities of PE-*b*-PPE polymeric micelles to HeLa cells were evaluated using the MTT method. Figure 11 shows the cell viability after 24h incubation with micelles of PE_{680}-*b*-$PEEP_{170}$ and PE_{680}-*b*-$PMeEP_{112}$ micelles in a concentration range of 50-1000 μg/mL. The cell viability in the presence of various concentrations of PE-*b*-PPE micelles was in the range from 101±3% to 88±6% in relation to untreated cells. This result demonstrates that PE-*b*-PPE polymeric micelles exhibit very low cytotoxicity even at high concentration. In contrast to previous work on block copolymers with hydrophobic PCL,[57-59] our study reports the initial synthesis of new PE-*b*-PPE block copolymers by a new synthetic strategy combining living catalytic polymerization and ROP of cyclic phosphate monomers. More importantly, hydrophobic PE core endows PE-*b*-PPE polymeric micelles with high loading efficiency and content of PTX and prolonging release behavior.

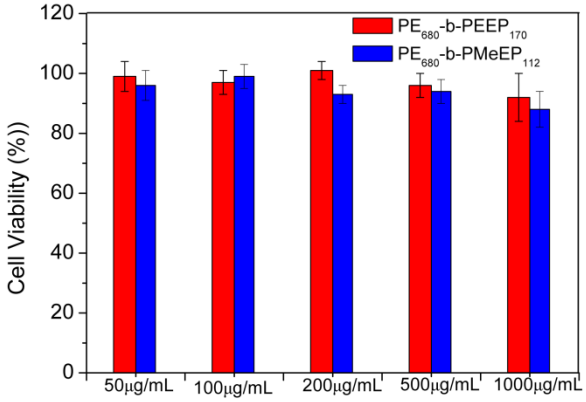

Figure 11 In vitro cell viability of HeLa cells treated with PE-*b*-PPE polymeric micelles after 24 h of incubation. Data were shown as mean ± S.D. (n = 3).

Experimental

General Procedures

All manipulations involving air- and moisture sensitive compounds were carried out under an atmosphere of dried and purified nitrogen with standard vacuum-line, Schlenk, or glovebox techniques.

Materials

Dichloromethane and chloroform were distilled from CaH_2 under nitrogen, and toluene and hexane from Na/K alloy. Ethylene (99.99%) was purified by passing through Agilent moisture and oxygen traps. Butane-2,3-dione, 2,6-diisopropylaniline, $ZnEt_2$ (1.0 M in toluene) and $(DME)NiBr_2$ were purchased from Aldrich and used as received. Modified methylaluminoxane (MMAO) (7 wt. % Al in heptane) was purchased from Akzo-Nobel and used as received. 1,8-Diazabicyclo[5.4.0]undec-7-ene (DBU) was purchased from Alfa Aesar and purified by recrystallization. Trimethylaluminium (TMA，2.0 M in toluene) was purchased from Acros. Amine-imine nickel complex $[Ar\text{-}N{=}C(Me)\text{-}(Me)_2C\text{-}NH\text{-}Ar]NiBr_2$ (Ar = 2,6-diisopropylphenyl) was synthesized according to our previously reported method.[21-27] Thiourea (TU) was synthesized according to a reported method.[60] 2-Ethyoxyl-2-oxo-1,3,2-dioxaphospholane[61] and 2-methyl-2-oxo-1,3,2-dioxaphospholane[52] were prepared according to literature methods (see supporting information). All solvents and other reagents if not specified were purchased from Sinopharm Chemical Reagent Co., Ltd. S. and purified by standard procedure.

Measurements

NMR spectra of organic compounds were carried out on a Bruker 500 MHz instrument in $CDCl_3$. Copolymer characterizations with gel permeation chromatography (GPC) were carried out on a Waters Breeze instrument system equipped a differential refractive index (DRI) detector (Waters 2417) with $CHCl_3$ as the eluant at a flow rate of 1.0 mL/min. Gel permeation chromatography (GPC) analysis of the molecular weight and molecular weight distribution (*Mw*/*Mn*) of the PE sample at 150 °C was performed on a high-temperature chromatography. PL-GPC 220 instrument equipped with a triple detection array, including a differential refractive index (DRI) detector, a two-angle light scattering (LS) detector (15, 90°), and a four-bridge capillary viscometer. The laser wavelength was 658 nm. 1,2,4-Trichlorobenzene (TCB) was used as the eluant at a flow rate of 1.0 mL/min. Laser light scattering experiments were carried out using a commercial spectrometer Brookhaven BI-200SM with a BI-9000AT digital correlator and a laser at λ = 532 nm. The samples were placed in an index-matching decalin bath with temperature control within (0.2 °C). Each solution was clarified by passing through a 0.45 μm PTFE filter to remove dust. The samples were equilibrated in the decalin bath at each temperature for 30 min before data collection. In dynamic light scattering (DLS), the cumulant analysis of the measured intensity-intensity time correlation function $G_2(t)$ of narrowly dispersed polymer chains in a dilute solution is sufficient to determine an accurate average line width (Γ). For a diffusive relaxation, Γ is related to the average translational diffusive coefficient by $D = \Gamma/q^2 q \rightarrow 0$ and the average hydrodynamic radius by $Rh = k_B T/6\pi\eta D$ with k_B, η, and T being the Boltzmann constant, the solvent viscosity, and the absolute temperature, respectively. Transmission electron microscopy (TEM)

observations were performed on a TEM (Philips TECNAI) with an accelerating voltage of 120 kV. To observe the original morphological sizes and geometries in aqueous solution, a drop from the previously prepared micelle solution was deposited onto a carbon-coated copper grid. After a few minutes, the excess solution was blotted away with filter paper. The morphological observations of the blend polymer were performed by frozen-section with a diamond knife at low temperature. All fluorescence spectra were recorded on a VARIAN Cary Eclipse fluorescence spectrophotometer. For encapsulating hydrophobic PTX drug test, the PTX concentration was measured with high-performance liquid chromatography (Agilent HP1100), and PTX was detected at a wavelength of 230 nm. Loading content and loading efficiencies were determined by applying the following equations: PTX Loading content = (weight of the loaded PTX/weight of the polymeric micelles) ×100%; PTX Loading efficiency = (amount of PTX in the polymeric micelles/initial amount of the PTX) × 100%. The concentration of the released PTX in the medium was analyzed by HPLC at 227 nm.

Polymerization of ethylene and synthesis of PE–OH

In a typical procedure, a round-bottom Schlenk flask with stirring bar was heated 3 h to 150 °C under vacuum and then cooled to room temperature. The flask was pressurized to 1 atm of ethylene and vented three times. The appropriate MMAO solution as a cocatalyst was introduced into the glass reactor under 0.2 atm (manometer pressure) of ethylene. The system was maintained by continuously stirring for 5 min, and then toluene and 2 mL solution of amine-imine nickel complex (360 μmol) in CH_2Cl_2 were syringed into the well-stirred solution in order, and the total reaction volume was kept at 240 mL. The ethylene pressure was kept a constant value of 0.2 atm throughout the reaction. The reaction temperature of 0 °C was maintained in polymerization experiment. After 10 minutes, the ethylene feed was stopped, and the reaction flask was charged with N_2 and vented for three times. Then $ZnEt_2$ solution (Zn/Ni = 100) was charged into reaction system, and the system was maintained by continuously stirring for 3 h at room temperature. Dry O_2 was introduced into solution, and oxidative workup was performed at 100 °C for 4 h. Finally, the reaction solution was poured into acidic methanol (95:5 methanol/HCl). The resulting precipitated polymers were collected and treated by filtration, washing with methanol several times, and drying in vacuum at 40 °C to a constant weight. The obtained PE is soluble in organic solvents such as petroleum ether, hexane, toluene, CH_3Cl, CH_2Cl_2, and trichlorobenzene because of high branching density. ^{1}H NMR ($CDCl_3$, ppm): 3.65 (t, 2H); 1.4-0.5 (PE). The chain end functionality is determined to be ~92% by a ratio of absolute M_n determined by GPC with a light scattering (LS) detector to the data detected by the ^{1}H NMR spectrum.

Synthesis of PE-*b*-PEEP block copolymers

A round-bottom Schlenk flask with stirring bar was heated 3 h to 150 °C under vacuum and then cooled to room temperature. The flask was pressurized to 1 atm of N_2 and vented three times. The appropriate PE–OH compound in 2 mL of dried THF as macroinitiator was introduced into the glass reactor under N_2. EEP monomer solution in dried THF, TU solution, and DBU were injected into the flask in order at 0 °C. After the polymerization reaction was maintained by continuously stirring for a desired time, the reaction was terminated by acidic THF solution (HAC/THF). The organic small molecules were removed by dialysis of the polymer product solution in THF. The resultant copolymer in the THF solution was poured into ethanol to remove PE homopolymer because introduction of PEEP block led to good solubility of copolymer in ethanol. The resulting block copolymers were collected by drying in vacuum at 40 °C to a constant weight.

Synthesis of PE-*b*-PMeEP block copolymers

A round-bottom Schlenk flask with stirring bar was heated 3 h to 150 °C under vacuum and then cooled to room temperature. The flask was pressurized to 1 atm of N_2 and vented three times. The appropriate PE–OH compound in 3.5 mL of dried $CHCl_3$ as macroinitiator was introduced into the glass reactor under N_2. MeEP monomer solution in dried $CHCl_3$ and DBU were injected into the flask in order at 0 °C. After the polymerization reaction was maintained by continuously stirring for a desired time, the reaction was terminated by acidic $CHCl_3$ solution (HAC/$CHCl_3$). The resultant product was purified by dialysis for removal of organic small molecule compounds. Then the polymer in the $CHCl_3$ solution was poured into ethanol to remove PE homopolymer. The resultant copolymers were collected by drying in vacuum at 40 °C to a constant weight.

Preparation of PE-*b*-PPE polymeric micelles

Solutions of the PE-*b*-PPE amphiphiles in THF were prepared by direct dissolution in THF at room temperature for 72 h in a vessel. Aqueous solution of the copolymers was prepared by dialysis of the solution in good solvent THF against water for 5 days at 25 °C. The aqueous solutions were allowed to equilibrate for at least 3 days under condition of 25 °C before use. All follow-up self-assembly experiments of the block copolymers were performed above the critical aggregation concentrations (CAC).

Preparation of paclitaxel-loaded micelles

Paclitaxel-loaded PE-b-PPE micelles were prepared by the dialysis method. The block copolymer was dissolved in THF, and paclitaxel was subsequently added with varying feed weight ratio to block copolymer. The solution was then stirred for 12 h at room temperature and was dialyzed using a membrane against distilled water. After 40 h dialysis, the solution was centrifuged at 10,000 g for 30 min to remove unloaded paclitaxel precipitates. The supernatant was filtered through a 0.2 μm membrane filter, followed by lyophilization. The loading efficiency and content of paclitaxel in micelles was measured by HPLC after the disruption of micelles and the solubilization of paclitaxel in acetonitrile.

Cytotoxicity assay

HeLa cell lines were provided by the center of experimental animals Sun Yat-Sen University (China). Those cell lines were maintained in folate-free RPMI 1640 media (Gibco Co., USA) supplemented with penicillin, streptomycin, and 10% fetal bovine serum (FBS) and in a humidified atmosphere containing 5% CO_2 at 37 °C. The cytotoxicity was evaluated by MTT assay. HeLa cells were seeded at 7.5×10^3 cells per well density in folate-free RPMI 1640 media. The medium was incubated at 37 °C, 5% CO_2 for 24 h, and then was replaced with 200 μL RPMI 1640 media containing FEG micelles without drug in the concentration range from 50 to 1000 μg/mL. After 24 h of incubation, the medium of each well was added with 20 μL MTT solution (5 mg/mL). After another 4 h of incubation, the medium of each well was replaced with 200 μL DMSO. Finally, the cell viability was analyzed by an ELISA reader (Bio-Rad, USA) at 570 nm. The values represent the mean ± SD of 3 replicates and were plotted relative to the untreated cells.

Conclusions

In conclusion, we report the initial synthesis and characterization of well-defined PE-*b*-PEEP and PE-*b*-PMeEP diblock copolymers by a sequential synthetic strategy combining living polymerization of ethylene and ring-opening polymerization of cyclic phosphoester monomers. The functionalization that we describe here provides a viable access to precisely constructing functional PE material by transition metal catalyzed living polymerization of ethylene followed by other controlled polymerization fashions. The novel amphiphilic PE-*b*-PPE block copolymers can self-assemble into spherical micelles in aqueous solution, and the size of the aggregate can be manipulated by tuning the chain length of PPE. PE-*b*-PPE polymeric micelles can efficiently carry PTX drug, hydrophobic PE core endows PE-*b*-PPE polymeric micelles with high loading efficiency and content of PTX and prolonging release behavior. The obtained functional PE also opens new potential applications of polyolefin materials in the areas of controlled drug delivery and release and biomaterials.

Acknowledgements

This work was supported by grants from National Natural Science Foundation of China (NSFC) (Projects 21174164, 51173209, 21274167, and 21374134), Natural Science Foundation of Guangdong Province (1414050000552), Technology Innovation Project of Educational Commission of Guangdong Province of China (2013KJCX0002), the Fundamental Research Funds for the Central Universities (15lgzd03), and CNPC Innovation Foundation (2014D-5006-0502).

Notes and references

1 R. Mülhaupt, *Macromol. Chem. Phys.*, 2003, **204**, 289-327.
2 T. C. Chung, Prog. Polym. Sci., 2002, **27**, 39-85.
3 M. J. Yanjarappa and S. Sivaram, *Prog. Polym. Sci.,* 2002, 27, 1347-1398.
4 R. Godoy Lopez, F. D'Agosto and C. Boisson, *Prog. Polym. Sci.*, 2007, **32**, 419-454.
5 D. A. Olson, L. Chen and M. A. Hillmyer, *Chem. Mater.*, 2008, **20**, 869-890.
6 Xu, Y.; Thurber, C. M.; Lodge, T. P.; Hillmyer, M. A. *Macromolecules,* **2012**, *45,* 9604-9610.
7 Y. Xu, C. M. Thurber, T. P. Lodge and M. A. Hillmyer, *Macromolecules*, 2012, **45**, 9604-9610.
8 K. Zhang, J. Wang, R. Subramanian, Z. Ye, J. Lu and Q. Yu, *Macromol. Rapid Commun.*, 2007, **28**, 2185-2191.
9 C. S. Popeney, M. C. Lukowiak, C. Böttcher, B. Schade, P. Welker, D. Mangoldt, G. Gunkel, Z. Guan and R. Haag, *ACS Macro Lett.*, 2012, **1**, 564-567.
10 G. Chen and Z. Guan, *J. Am. Chem. Soc.*, 2004, **126**, 2662-2663.
11 X. Shi, Y. Zhao, H. Gao, L. Zhang, F. Zhu and Q. Wu, *Macromol. Rapid Commun.*, 2012, **33**, 374-379.
12 H. Y. Gao, Y. Tang, Z. L. Hu, Q. R. Guan, X. B. Shi, F. M. Zhu and Q. Wu, *Polym. Chem.*, 2013, **4**, 1107-1114.
13 P. Alexandridis and B. Lindman, *Amphiphilic block copolymers: self-assembly and applications*, Elsevier, 2000 pp. 1-448.
14 M. M. Hasani-Sadrabadi, V. Karimkhani, F. S. Majedi, J. J. Van Dersarl, E. Dashtimoghadam, F. Afshar-Taromi, H. Mirzadeh, J. Bertsch, K. I. Jacob, P. Renaud, F. J. Stadler and I. Kim, *Adv. Mater.*, 2014, **26**, 3118-3123..
15 S. J. Holder and N. A. J. M. Sommerdijk, *Polym. Chem.*, 2011, **2**, 1018-1028.
16 F. Chécot, S. Lecommandoux, Y. Gnanou and H.-A. Klok, *Angew. Chem. Int. Ed.*, 2002, **41**, 1339-1343.
17 H. Kukula, H. Schlaad, M. Antonietti and S. Förster, *J. Am. Chem. Soc.*, 2002, **124**, 1658-1663
18 R. Sigel, M. Łosik and H. Schlaad, *Langmuir*, 2007, **23**, 7196-7199.
19 T. Li, W. J. Wang, R. Liu, W. H. Liang, G. F. Zhao, Z. Li, Q. Wu and F. M. Zhu, *Macromolecules*, 2009, **42**, 3804-3810.
20 Y. Zhao, X. B. Shi, H. Y. Gao, L. Zhang, F. M. Zhu and Q. Wu, *J. Mater. Chem.*, 2012, **22**, 5737-5745.
21 Y. Zhao, H. Gao, G. Liang, F. Zhu and Q. Wu, *Polym. Chem.*, 2014, **5**, 962-970.
22 H. Gao, Z. Hu, Q. Guan, Y. Liu, F. Zhu and Q. Wu, *Polymer*, 2013 **54**, 4923-4929.
23 H. Gao, G. Li, Z. Hu, Z. Xiao, G. Liang and Q. Wu, *Polymer*, 2014, **55**, 4593-4600.
24 Z. Zhang and Z. Ye, *Chem. Commun.*, 2012, **48**, 7940-7942.
25 L. Xu and Z. Ye, *Chem. Commun.*, 2013, **49**, 8800-8802.
26 Z. Ye, L. Xu, Z. Dong and P. Xiang, *Chem. Commun.*, 2013, **49**, 6235-6255.
27 Z. Dong and Z. Ye, *Polym. Chem.*, 2012, **3**, 286-301.
28 H. Gao, H. Hu, F. Zhu and Q. Wu, *Chem. Commun.*, 2012, **48**, 3312-3314
29 H. Hu, L. Zhang, H. Gao, F. Zhu and Q. Wu, *Chem. Eur. J.*, 2014, **20**, 3225-3233
30 S. Zai, F. Liu, H. Gao, C. Li, G. Zhou, S. Cheng, L. Guo, L. Zhang, F Zhu and Q. Wu, *Chem. Commun.*, 2010, **46**, 4321-4323.
31 S. Zai, H. Gao, Z. Huang, H. Hu, H. Wu and Q. Wu, *ACS. Cata* 2012, **2**, 433-440.
32 H. Hu, H. Gao, D. Chen, G. Li, Y. Tan, G. Liang, F. Zhu and Q. Wu, *ACS. Catal.*, 2015, **5**, 122-128.
33 J. Liu, W. Huang, Y. Pang, X. Zhu, Y. Zhou and D. Yan, *Langmu* 2010, **26**, 10585-10592.
34 Z. Zhao, J. Wang, H.-Q. Mao and K. W. Leong, *Adv. Drug D l. Rev.*, 2003, **55**, 483-499.

35 C.-S. Xiao, Y.-C. Wang, J.-Z. Du, X.-S. Chen and J. Wang, *Macromolecules*, 2006, **39**, 6825-6831.
36 Y. Iwasaki, C. Wachiralarpphaithoon and K. Akiyoshi, *Macromolecules*, 2007, **40**, 8136-8138.
37 Y.-C. Wang, S.-Y. Shen, Q.-P. Wu, D.-P. Chen, J. Wang, G. Steinhoff and N. Ma, *Macromolecules*, 2006, **39**, 8992-8998.
38 J.-Z. Du, D.-P. Chen, Y.-C. Wang, C.-S. Xiao, Y.-J. Lu, J. Wang and G.-Z. Zhang, *Biomacromolecules*, 2006, **7**, 1898-1903.
39 Y.-C. Wang, Y. Li, X.-Z. Yang, Y.-Y. Yuan, L.-F. Yan and J. Wang, *Macromolecules*, 2009, **42**, 3026-3032.
40 R. Kempe, *Chem. Eur. J.*, 2007, **13**, 2764-2773.
41 R. Briquel, J. Mazzolini, T. Le Bris, O. Boyron, F. Boisson, F. Delolme, F. D'Agosto, C. Boisson and R. Spitz, *Angew. Chem. Int. Ed.*, 2008, **47**, 9311-9313.
42 W. Zhang and L. R. Sita, *J. Am. Chem. Soc.*, 2007, **130**, 442-443.
43 Y.-C. Wang, L.-Y. Tang, Y. Li and J. Wang, *Biomacromolecules*, 2008, **10**, 66-73.
44 W.-J. Song, J.-Z. Du, N.-J. Liu, S. Dou, J. Cheng and J. Wang, *Macromolecules*, 2008, **41**, 6935-6941.
45 Y.-C. Wang, Y. Li, X.-Z. Yang, Y.-Y. Yuan, L.-F. Yan and J. Wang, *Macromolecules*, 2009, **42**, 3026-3032.
46 J. Liu, Y. Pang, W. Huang, X. Zhai, X. Zhu, Y. Zhou and D. Yan, *Macromolecules*, 2010, **43**, 8416-8423.
47 Y. Iwasaki and E. Yamaguchi, *Macromolecules*, 2010, **43**, 2664-2666.
48 S. Zhang, A. Li, J. Zou, L. Y. Lin and K. L. Wooley, *ACS Macro Lett.*, 2012, **1**, 328-333.
49 S. Zhang, J. Zou, F. Zhang, M. Elsabahy, S. E. Felder, J. Zhu, D. J. Pochan and K. L. Wooley, *J. Am. Chem. Soc.*, 2012, **134**, 18467-18474.
50 S. Zhang, H. Wang, Y. Shen, F. Zhang, K. Seetho, J. Zou, J.-S. A. Taylor, A. P. Dove and K. L. Wooley, *Macromolecules*, 2013, **46**, 5141-5149.
51 B. Clément, B. Grignard, L. Koole, C. Jérôme and P. Lecomte, *Macromolecules*, 2012, **45**, 4476-4486.
52 T. Steinbach, S. Ritz and F. R. Wurm, *ACS Macro Lett.*, 2014, **3**, 244-248.
53 H. Aranda-Espinoza, H. Bermudez, F. S. Bates and D. E. Discher, *Phys. Rev. Lett.*, 2001, **87**, 208301.
54 D. E. Discher and A. Eisenberg, *Science*, 2002, **297**, 967-973.
55 R. R. Sawant, O. S. Vaze, K. Rockwell, V. P. Torchilin, *Eur. J. Pharm. Biopharm.* 2010, **75**, 321-326
56 Z. Du , S. Pan , Q. Yu , Y. Li , Y. Wen , W. Zhang , M. Feng , C. Wu , *Coll. Surf. A: Physicochem. Eng. Aspects* 2010, **353**, 140-148.
57 Y. Wang, L. Tang, T. Sun, C. Li, M. Xiong, and J. Wang, *Biomacromolecules* 2008, **9**, 388-395.
58 E. K. Park, S. B. Lee and Y. M. Lee, *Biomaterials*, 2005, **26**, 1053-1061.
59 S. Cheon Lee, C. Kim, I. Chan Kwon, H. Chung and S. Young Jeong, *J. Controlled Release*, 2003, **89**, 437-446.
60 R. C. Pratt, B. G. G. Lohmeijer, D. A. Long, P. N. P. Lundberg, A. P. Dove, H. Li, C. G. Wade, R. M. Waymouth and J. L. Hedrick, *Macromolecules*, 2006, **39**, 7863-7871.
61 J. Libiszowski, K. Kałużynski and S. Penczek, *J. Polym. Sci., Part A: Polym. Chem.*, 1978, **16**, 1275-1283.